Biochimica et Biophysica Acta 1838 (2014) 2260–2268

Contents lists available at ScienceDirect

Biochimica et Biophysica Acta

journal homepage: www.elsevier.com/locate/bbamem

# $^{19}$F NMR screening of unrelated antimicrobial peptides shows that membrane interactions are largely governed by lipids ☆

Sergii Afonin [a], Ralf W. Glaser [b], Carsten Sachse [c], Jesús Salgado [d], Parvesh Wadhwani [a], Anne S. Ulrich [a,e,*]

[a] Karlsruhe Institute of Technology (KIT), Institute of Biological Interfaces (IBG-2), POB 3640, 76021 Karlsruhe, Germany
[b] Institute of Biochemistry and Biophysics, Friedrich-Schiller-Universität Jena, Hans-Knöll-Str. 2, 07745 Jena, Germany
[c] EMBL — European Molecular Biology Laboratory, Structural and Computational Biology, Meyerhofstr. 1, 69117 Heidelberg, Germany
[d] Institute of Molecular Science (ICMol), University of Valencia, C/Catedrático José Beltrán, 2, 46980 Paterna, Valencia, Spain
[e] Karlsruhe Institute of Technology (KIT), Institute of Organic Chemistry, Fritz-Haber-Weg 6, 76131 Karlsruhe, Germany

ARTICLE INFO

*Article history:*
Received 13 January 2014
Received in revised form 23 March 2014
Accepted 24 March 2014
Available online 31 March 2014

*Keywords:*
Amphiphilic antimicrobial peptides
Re-alignment in membrane
Solid state $^{19}$F NMR structure analysis
Lipid composition
Bacterial membranes
Spontaneous curvature

ABSTRACT

Many amphiphilic antimicrobial peptides permeabilize bacterial membranes *via* successive steps of binding, re-alignment and/or oligomerization. Here, we have systematically compared the lipid interactions of two structurally unrelated peptides: the cyclic β-pleated gramicidin S (GS), and the α-helical PGLa. $^{19}$F NMR was used to screen their molecular alignment in various model membranes over a wide range of temperatures. Both peptides were found to respond to the phase state and composition of these different samples in a similar way. In phosphatidylcholines, both peptides first bind to the bilayer surface. Above a certain threshold concentration they can re-align and immerse more deeply into the hydrophobic core, which presumably involves oligomerization. Re-alignment is most favorable around the lipid chain melting temperature, and also promoted by decreasing bilayer thickness. The presence of anionic lipids has no influence in fluid membranes, but in the gel phase the alignment states are more complex. Unsaturated acyl chains and other lipids with intrinsic negative curvature prevent re-alignment, hence GS and PGLa do not insert into mixtures resembling bacterial membranes, nor into bacterial lipid extracts. Cholesterol, which is present in high concentrations in animal membranes, even leads to an expulsion of the peptides from the bilayer and prevents their binding altogether. However, a very low cholesterol content of 10% was found to promote binding and re-alignment of both peptides. Overall, these findings show that the ability of amphiphilic peptides to re-align and immerse into a membrane is determined by the physico-chemical properties of the lipids, such as spontaneous curvature. This idea is reinforced by the remarkably similar behavior observed here for two structurally unrelated molecules (with different conformation, size, shape, charge), which further suggests that their activity at the membrane level is largely governed by the properties of the constituent lipids, while the selectivity towards different cell types is additionally ruled by electrostatic attraction between peptide and cell surface. This article is part of a Special Issue entitled: Interfacially Active Peptides and Proteins. Guest Editors: William C. Wimley and Kalina Hristova.



## 1. Introduction

All multicellular organisms rely on antimicrobial peptides (AMPs) as part of their innate immune response [1–7]. Besides their activity against bacteria, some AMPs can also lyse enveloped viruses, fungi, and even tumor cells [1,2,8,9]. The peptides are usually short, amphiphilic, and generally cationic, but they are unrelated with regard to other structural or genetic features. Their primary target is the bacterial

*Abbreviations:* NMR, nuclear magnetic resonance spectroscopy; GS, gramicidin S; AMP, antimicrobial peptide(s); $CF_3$-Phg, CF3-phenylglycine or 2-Amino[4-(trifluoromethyl)phenyl] acetic acid; 4F-Phg, 4F-phenylglycine or 2-Amino-2-(4-fluorophenyl)acetic acid; $CF_3$-Bpg, CF3-bicyclopentylglycine or 2-Amino-2-[3-(trifluoromethyl)bicyclo[1.1.1]pent-1-yl]ethanoic acid; RP-HPLC, reverse-phase high-performance liquid chromatography; MALDI-TOF, matrix-assisted laser induced desorption/ionization (mass spectroscopy) with time-of-fly detection; DLPC, 1,2-dilauroyl-*sn*-glycero-3-phosphocholine; DPPC, 1,2-dipalmitoyl-*sn*-glycero-3-phosphocholine; DOPC, 1,2-dioleoyl-*sn*-glycero-3-phosphocholine; DMPC, 1,2-dimyristoyl-*sn*-glycero-3-phosphocholine; DMPG, 1,2-dimyristoyl-*sn*-glycero-3-phospho-(1′-*rac*-glycerol); DMPS, 1,2-dimyristoyl-*sn*-glycero-3-phospho-*L*-serine; DMPE, 1,2-dimyristoyl-*sn*-glycero-3-phosphoethanolamine; POPE, 1-palmitoyl-2-oleoyl-*sn*-glycero-3-phosphoethanolamine; *E. coli* TLE, total lipid extract from *Escherichia coli*; MeOH, $CH_3OH$; P/L, peptide-to-lipid (molar) ratio; $T_m$, acyl chain melting (phase) transition of a phospholipid; $\delta_{iso}$, isotropic NMR frequency; CHOL, (3β)-cholest-5-en-3-ol; CL, cardiolipin(s); ER, endoplasmic reticulum; MIC, minimum inhibitory concentration.

☆ This article is part of a Special Issue entitled: Interfacially Active Peptides and Proteins. Guest Editors: William C. Wimley and Kalina Hristova.

* Corresponding author at: Karlsruhe Institute of Technology (KIT), Institute of Organic Chemistry, Fritz-Haber-Weg 6, 76131 Karlsruhe, Germany. Tel.: +49 721 60843222; fax: +49 721 60844823.
*E-mail address:* Anne.Ulrich@kit.edu (A.S. Ulrich).

http://dx.doi.org/10.1016/j.bbamem.2014.03.017
0005-2736/

cell membrane, hence AMPs may have a potential to overcome the problem of acquired antibiotic resistance. Since activity was found to occur in a non-sterospecific manner, it was concluded that these peptides physically permeabilize and/or penetrate the lipid envelope of the bacteria [10–13]. To rationalize their molecular mechanisms in terms of peptide–lipid interactions, let us consider the relevant parameters which determine the equilibria of (i) peptide binding to the membrane surface, (ii) re-alignment and deeper immersion into the bilayer, and finally (iii) membrane rupture. These successive steps are obviously influenced by both, the type of peptide as well as the lipid composition. It is well recognized that anionic bacterial membranes have a high electrostatic affinity for cationic AMPs (step i), whereas uncharged eukaryotic membranes with a high cholesterol content are more resilient to antimicrobial attack (steps ii and iii) [13–16]. Here, we will demonstrate for two completely unrelated AMPs that the second step (ii) of re-alignment and bilayer immersion is consistently and quantitatively governed by the lipids, independent of peptide sequence, secondary structure or charge. The only relevant parameter to be considered here for each individual peptide is the actual threshold concentration at which it will start to re-align. When studying the system under conditions close to this threshold, we will see that the equilibrium gets shifted by the different lipid environments in a consistent manner, irrespective of the peptide itself.

The well-known concept of Shai–Matsuzaki–Huang describes how amphiphilic peptides bind to and immerse into a lipid bilayer, thereby disrupting its integrity [17–19]. Permanent or transient self-assembly of the peptides can lead to a transmembrane pore, *e.g.* a "barrel-stave" or "toroidal wormhole", and non-specific bilayer rupture can occur *e.g. via* a "carpet" mechanism. From a structural point of view, these situations can be described in terms of rigid bodies (unless unfolding and/or aggregation events have to be considered) [20–22]. The amphiphilic molecules are simply characterized by their alignment in the membrane, and by their mobility and oligomeric state. Solid state NMR in macroscopically aligned samples has been established as a routine method to characterize such peptides carrying selective isotope labels ($^{2}$H, $^{13}$C, $^{15}$N, $^{19}$F) [23–30]. $^{31}$P NMR is conveniently used to monitor the state of the lipids [23,31,32]. Numerous AMPs have thus been studied in model membranes of varying composition [29,30,33–35]. However, it is very difficult to compare these data with one another, because the exact sample conditions are known to have a dramatic impact on peptide behavior. In a comprehensive series of experiments it has been systematically described how the representative antimicrobial peptide PGLa changes its membrane alignment, dynamics and oligomerization state, not only as a function of concentration, but also as a function of lipid composition, temperature, sample hydration, pH, and in the presence of other peptides [27,36–43]. Furthermore, a recent study has shown that re-alignment of the related peptide MSI-103 is governed by the spontaneous membrane curvature [44].

To elucidate the fundamental role of physico-chemical lipid properties and membrane composition, it is essential to study different AMPs under identical conditions, based on the same sample preparation protocol and experimental set-up. Here, we have systematically characterized and compared two structurally unrelated AMPs in various lipid environments in a parallel manner. Two aspects are of particular novelty: (i) a single fluorine-label was used as a $^{19}$F NMR reporter group to probe the orientation and re-alignment of the GS and PGLa, as the complete structures and alignment states are already known for both peptides from previous reports [36,37,41,27,45,46]; (ii) instead of focusing only on a single temperature, the method is sensitive enough to run extensive temperature series encompassing both the gel state and the fluid liquid crystalline phases of the different membrane systems. Even though this rapid screening approach is based on spectra with relatively low quality, the present solid state $^{19}$F NMR study adds two further supportive examples to our recent concept of lipid–protein interactions. In a systematic analysis of the related α-helical peptide MSI-103, we had demonstrated for a wide range of different lipids that peptide re-alignment and membrane insertion are governed simply by the spontaneous curvature of the lipid bilayer [44].

PGLa (GMASKAGAIAGKIAKVALKAL-$NH_2$) is a member of the magainin family of antimicrobial peptides, isolated from the skin of the African clawed frog *Xenopus laevis* [47]. It is unstructured in solution, but folds into an amphiphilic α-helix upon binding to a lipid bilayer, with a net charge of +5. In DMPC and in the presence of negatively charged DMPG, the cationic peptide was shown to re-align in a concentration-dependent manner from a surface-bound "S-state" to an obliquely tilted "T-state" [36–38]. The latter state has been attributed to antiparallel homodimers, which are more deeply immersed in the hydrophobic bilayer core [48,49]. When the membrane is cooled down to the gel phase, PGLa can re-align even further into a completely inserted "I-state", which presumably corresponds to an oligomeric transmembrane pore [41]. In the presence of its synergistic partner peptide Magainin 2, this stable I-state has been observed for PGLa even in the fluid liquid crystalline phase of DMPC/DMPG [39,42,43]. In the following, we will refer to both the T-state and the I-state of PGLa as "re-aligned", to be differentiated from the original surface-bound S-state.

The second peptide investigated here is gramicidin S (GS, *cyclo*[Pro-Val-Orn-Leu-$^{D}$Phe]$_2$; Orn: ornithine, $^{D}$Phe: (*D*)-phenylalanine) from *Aneurinibacillus migulanus* (formerly known as *Bacillus brevis*) [50], which represents one of the few AMPs already in use as an antibiotic drug [51,52]. This cationic decapeptide has a symmetric cyclic β-pleated structure with an amphiphilic character and a net charge of +2. In DMPC/DMPG membranes, GS first binds to the membrane surface, but it can re-align and flip into the hydrophobic core as a function of concentration and temperature. The membrane-inserted state has been suggested to form a transmembrane pore, consisting of an oligomeric β-barrel [27,45,46]. The structures and re-alignment transitions of both, PGLa and GS, have been comprehensively characterized by solid state $^{19}$F NMR in macroscopically oriented membrane samples [27–30,35–42,45,46,53–55], and $^{2}$H NMR was used to justify the viability of the $^{19}$F-labeling strategy [56]. In these previous investigations, the non-natural amino acids $CF_3$-phenylglycine ($CF_3$-Phg), 4F-phenylglycine (4F-Phg), or $CF_3$-bicyclopentylglycine ($CF_3$-Bpg), were used as $^{19}$F NMR reporters. In PGLa, a single $^{19}$F-labeled amino acid had been substituted one-by-one for positions Ile9, Ala10, Ile13, or Ala14. In gramicidin S, either the pair of Leu or of Val residues had been double-labeled. These selective substitutions affected neither the structure nor the antimicrobial activity of the peptide analogues [27,28,45,46,54,55]. This way, the structures and re-alignment behavior of membrane-bound PGLa and GS have been described from a combination of several individual NMR labels in previous works. On this basis, it is now possible to select a single $^{19}$F-labeled position on each peptide to serve as a fingerprint for identifying the different alignment states that are functionally relevant. Namely, for PGLa the $CF_3$-Phg label in position of Ile13 is ideally suited to discriminate between the surface-bound and the re-aligned states [41,53,57]. In the case of GS, the $^{19}$F NMR signal of 4F-Phg in place of Leu is a characteristic marker to observe re-alignment [27,29,30,45,46].

Here, we have monitored and compared the re-alignment of the selected $^{19}$F-labeled analogues of PGLa and GS in several different types of model membranes. This way, it should be possible to correlate their structural behavior with the role of lipid composition and other parameters under equivalent conditions. These new data thus extend our previous analyses of PGLa and GS, which had been carried out mainly as a function of concentration and temperature in DMPC and DMPC/DMPG [36,37,41,45,46]. Now, the peptides are systematically examined and compared further in (i) other saturated lipids with varying acyl chain length, (ii) bilayers with unsaturated acyl chains, (iii) bilayers with varying content of anionic head groups, (iv) bilayers with varying amounts of cholesterol, and (v) lipid mixtures with typical bacterial lipid compositions.

## 2. Material and methods

### 2.1. Peptide synthesis and purification

All peptides were synthesized using Fmoc-strategy according to published procedures [54,28,58]. In PGla, Ile13 was substituted with L-4-$CF_3$-phenylglycine to give Gly-Met-Ala-Ser-Lys-Ala-Gly-Ala-Ile-Ala-Gly-Lys-($CF_3$-Phg)-Ala-Lys-Val-Ala-Leu-Lys-Ala-Leu-$NH_2$. For GS, 4F-phenylglycine was used as a $^{19}$F-label in place of Leu, thus yielding the analogue *cyclo*[Pro-Val-Orn-(4F-Phg)-$^{D}$Phe]$_2$. Starting off with the racemic (D/L) $CF_3$-Phg amino acid, the respective peptide diastereomers were purified by RP-HPLC on Grace Vydac C18 columns (10 × 250 mm) using individually adjusted linear $H_2O$/acetonitrile gradients. The mobile phase contained 5 mM HCl instead of TFA to ensure a $^{19}$F-free background for NMR [54]. Analytical RP-HPLC (Grace Vydac C18: 4.6 × 250 mm column) and MALDI-TOF (Biflex III, Bruker) were used to identify the peptides and characterize their purity [54,58].

### 2.2. NMR sample preparation

The lipids DLPC, DPPC, DOPC, DMPC, DMPG, DMPS, DMPE, POPE, and total *E. coli* lipid extract (TLE) were obtained from Avanti Polar Lipids, cholesterol was from Sigma-Aldrich. Appropriate amounts of peptides and lipids were separately weighed out as dry powders, using a Mettler-Toledo microbalance. Next, stock solutions were prepared in a MeOH/$CHCl_3$ solvent mixture (about 2:1). The aliquots were combined to achieve the desired peptide-to-lipid ratio in a single vessel for each sample. These mixed solutions were used to prepare macroscopically oriented lipid bilayers on glass supports and hydrated *via* water vapor of 96% relative humidity, as previously described [36,37,45,46].

### 2.3. Solid state $^{19}$F and $^{31}$P NMR

All spectra were acquired on 500 MHz Unity (Varian) or Avance III (Bruker) spectrometers at 202.5 MHz ($^{31}$P) and 472 MHz ($^{19}$F). Either a Hahn-Echo ($^{31}$P, and $^{19}$F chemical shift anisotropy in GS) or a single 90° pulse ($^{19}$F dipolar coupling in PGLa) were applied with $^{1}$H-decoupling (for $^{19}$F-observation) as described earlier [36,37,45,46,54]. Care was taken to prevent dehydration of the samples (as monitored by $^{31}$P NMR) by wrapping them in plastic film and, if necessary, re-hydration and re-measuring [41,53]. Temperature control units from Varian/Bruker were used, and the respective probeheads were carefully calibrated externally using the $^{1}$H NMR thermometer [59]. Temperature-dependent measurements were performed by scanning upwards from at least 10° below the lipid phase transition temperature $T_m$ to at least 10° above $T_m$ in steps of 5°. Samples, placed such that their membrane normal is parallel to B0(horizontal membrane), were equilibrated for at least 10 min at each temperature (typically for 30 min). The $^{19}$F NMR spectra were externally referenced using an aqueous solution of 100 mM NaF, the resonance of which was set to −119.5 ppm at 35 °C [60], and for $^{31}$P NMR calibration with the primary reference of 85% $H_3PO_4$ was used.

## 3. Results

### 3.1. Characteristic alignment states of PGLa and GS in DMPC

Fig. 1 illustrates some representative $^{19}$F NMR spectra from our previous studies of PGLa and GS, which are used here to distinguish the

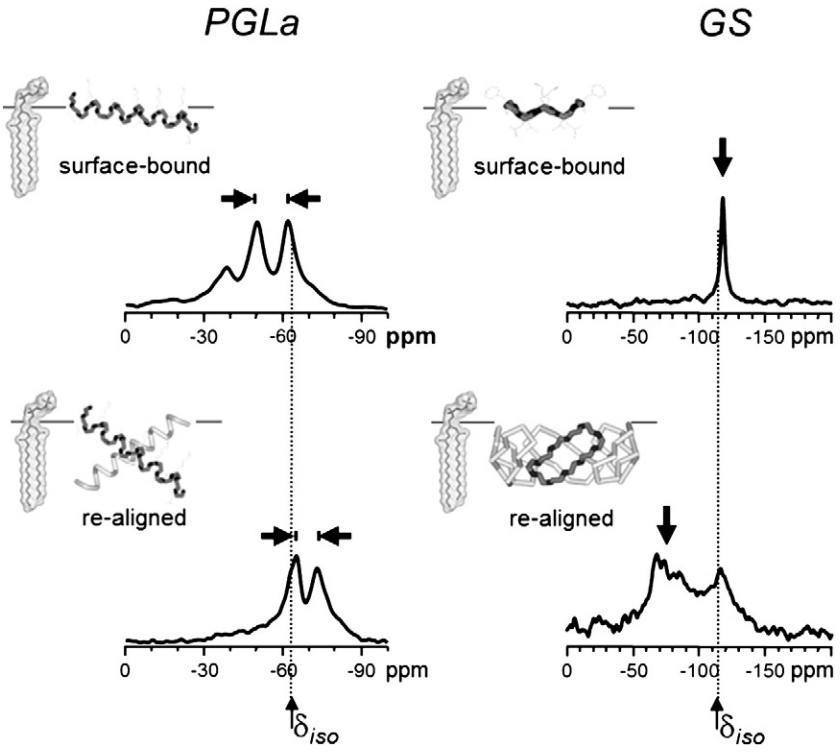


**Fig. 1.** Characteristic solid state $^{19}$F NMR fingerprint spectra of $^{19}$F-labeled PGLa (left, with $CF_3$-Phg in place of Ile13) and GS (right, with 4F-Phg in place of Leu), in macroscopically oriented DMPC bilayers. The molecular structures of the two amphiphilic peptides and their respective alignments in a horizontal membrane are illustrated besides each spectrum, *i.e.* the surface-bound states (top) and the re-aligned states (bottom). Arrows indicate the $^{19}$F dipolar coupling of PGLa (only one splitting indicated within the triplet), and the chemical shift of GS relative to the isotropic frequency $\delta_{iso}$ (dotted line). The spectral intensity in these regions serves as a fingerprint to identify the alignment state of each peptide. We note that PGLa has a characteristic downfield signature in the surface-bound state, while it shows upfield signals upon re-alignment. GS has a near-isotropic signal in the surface-bound state, and re-alignment produces intensity at the downfield edge of the spectrum. As outlined below, these peptides can reversibly change their alignment states as a function of concentration, temperature, and lipid composition.

surface-bound states from the re-aligned states. Both PGLa and GS yield distinctly different lineshapes in their two functionally relevant states. More detailed information on the interpretation of these data can be found in previous publications [27,36,37,41,45,46]. Here, we just give a brief description of the spectral features and their meaning. For PGLa, the $^{19}$F dipolar coupling of the selected "fingerprint" $CF_3$-label gives a positive +5.7 kHz splitting in the surface-bound state, which changes to a negative value upon re-alignment (−2.9 Hz in the tilted T-state, and −4.0 Hz in the inserted I-state [41]). It is the sign that matters here, and it can be read out by simple inspection of the PGLa spectra. Downfield signals, to the left of the isotropic frequency $\delta_{iso}$ (indicated as a dotted line) have a positive splitting and represent the S-state, while upfield signals to the right of $\delta_{iso}$ have a negative splitting and represent a re-aligned state of PGLa [36,37]. In gramicidin S, the chemical shift of the "fingerprint" $^{19}$F-labels changes from a narrow peak near $\delta_{iso}$ in the surface-bound state (−118 ppm), to a broad downfield signal upon re-alignment (−70 to −80 ppm, near the edge of the powder pattern) [27,45,46]. The convenient aspect in the choice of these fingerprint signals is that for both, PGLa and GS, the $^{19}$F NMR signals move far across the spectral width, and they can be readily assessed relative to the well-defined isotropic frequency $\delta_{iso}$.

While both peptides are monomeric in the surface-bound state, their re-alignment and membrane immersion have been suggested to be accompanied by self-assembly, yielding a dimer in the case of PGLa [37,48], and a β-barrel for GS [46]. We also infer for both peptides that they penetrate more deeply into the hydrophobic bilayer core upon re-alignment, which is supposedly the most critical step towards membrane permeabilization [37,41]. From the corresponding $^{31}$P NMR analyses of the lipid matrix, it is known that the bilayers remain lamellar and well oriented. Also in this work ($^{31}$P NMR data not shown), non-lamellar isotropic or hexagonal lipid signals were generally absent (except for some cubic morphologies observed in the bacterial total lipid extract preparations). Under the conditions used in this study, neither PGLa nor GS can thus induce the formation of micelles or non-bilayer phases in the macroscopically oriented and well hydrated membranes.

### 3.2. Peptide re-alignment as a function of concentration and temperature

For a systematic investigation, we first have to select a suitable range of peptide concentrations and temperatures, at which the functionally relevant re-alignment of PGLa and GS can be observed. We therefore repeated and reproduced the previously published concentration series for both peptides in DMPC under uniform conditions of sample preparation and experimental set-up [27,37,53]. Samples were prepared with peptide-to-lipid (P/L) molar ratios of 1:20, 1:35, 1:50, 1:80, 1:100, 1:150, 1:200, and 1:400 for PGLa, and 1:20, 1:40, 1:80 and 1:200 for GS. From these series, a representative set of $^{19}$F NMR spectra (all measured at 25 °C) has been selected for illustration in Fig. 2A. Both peptides are seen to be surface-bound at low concentration (downfield signals for PGLa, and near-isotropic signal for GS) up to a certain threshold, above which the re-alignment starts to occur (upfield signals for PGLa, and downfield signal for GS). The re-alignment of PGLa involves an equilibrium between the two discrete states [39], and fast exchange gives rise to a time-averaged signal at the isotropic position (around P/L ≈ 1:100) [37]. The immersed state is reached at P/L ≈ 1:50 for PGLa in DMPC. In the case of GS, the two states give rise to discrete signals, and the exchange seems to be slower. Hence, starting with the surface-bound state (signal near the isotropic position), an additional (downfield) signal corresponding to the re-aligned state starts to grow with increasing peptide concentration up to P/L ≈ 1:40. A certain fraction of the peptide is seen to remain in the surface-bound state even at higher concentrations. The behavior of both systems in Fig. 2A can thus be interpreted in terms of a concentration-dependent transition from a surface-bound state to a re-aligned state with increasing P/L ratio. PGLa is in fast exchange on the millisecond time scale of the dipolar coupling,

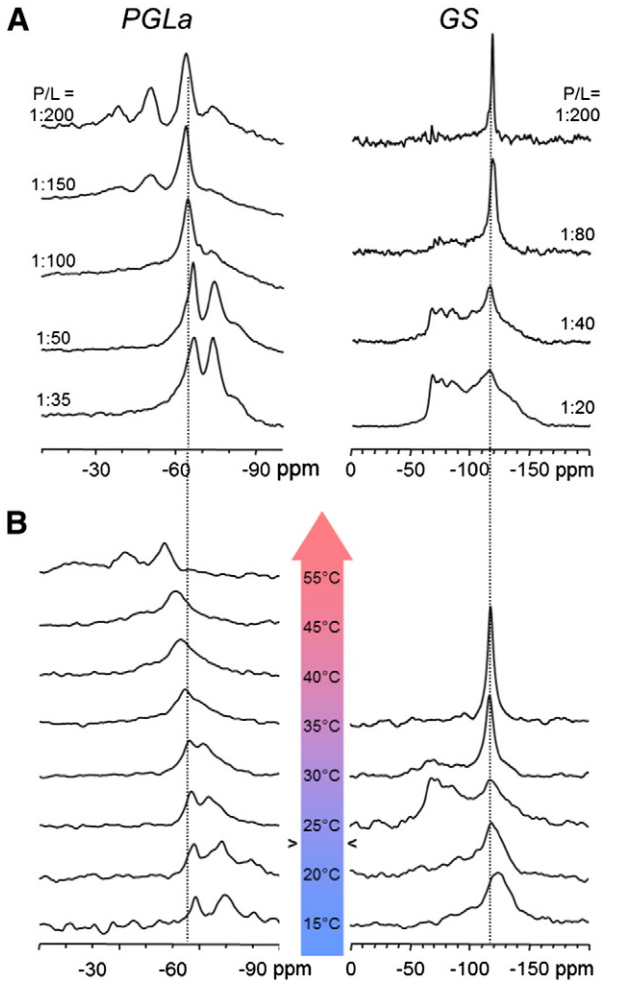


**Fig. 2.** (A) Concentration-dependent re-alignment of PGLa (left) and GS (right), as monitored by $^{19}$F NMR in oriented DMPC bilayers at 25 °C (1 mg lipid per glass slide, hydration at 96% relative humidity). The peptide-to-lipid molar ratio is indicated as P/L. (B) Re-alignment of PGLa (left, P/L = 1:50) and GS (right, P/L = 1:40) in DMPC, monitored as a function of temperature. The isotropic position is drawn as a dotted line in the spectra. The lipid acyl chain melting temperature is indicated by the arrow heads on the temperature scale.

while GS is in slow exchange. Re-alignment is complete at about 1:50 for PGLa and 1:40 for GS [40,46]. From these data we can identify the appropriate conditions for all further experiments, *i.e.* when each system is most sensitive to any factors that may affect the re-alignment equilibrium.[1] We thus selected the P/L ratios at which each peptide has just reached its re-aligned state in DMPC at 25 °C, namely at 1:50 for PGLa and 1:40 for GS. In all further experiments, these particular P/L ratios will be used to examine and compare the re-alignment behavior of the two peptides.

Next, we monitored the effect of the lipid phase state, by running heating scans over a broad range of temperatures around the acyl chain melting transition $T_m$ (23 °C). $^{19}$F NMR spectra were acquired in DMPC from 15 °C to 55 °C, as shown in Fig. 2B. In both systems we can discern three different temperature regimes that determine the alignment of the peptides: (i) well above the lipid phase transition, (ii) around and slightly above $T_m$, and (iii) well below $T_m$. For the sake of argument, we will discuss the classical "fluid" (liquid disordered) conditions first, before noting any observations in the biologically less relevant gel-phase. In the case of PGLa, the peptide is preferentially

[1] In this context it is important to note that the spectra in Fig. 2A were acquired at 25 °C, *i.e.* relatively close to the lipid chain melting transition of DMPC at $T_m$ ~23 °C, because in this region the re-alignment equilibrium is most pronounced and can be shifted by relatively weak effects.

surface-bound (downfield signals) in the fluid liquid crystalline phase at high temperatures (45–55 °C). Upon cooling, successive re-alignment occurs through fast exchange (isotropic signal at 35 °C, just like P/L = 1:100 in Fig. 2A) reaching the fully tilted state around $T_m$ (upfield signals). Below the lipid phase transition, PGLa remains in the tilted state [46]. In a similar way, GS prefers a surface-bound state at high temperatures (near-isotropic signal), while re-alignment into the membrane-immersed state is most pronounced around $T_m$ (downfield signals). In the lipid gel phase, on the other hand, GS produces a broad powder-like lineshape that indicates a lack of alignment, so the two peptides differ in this particular aspect. Nevertheless, we may altogether conclude that PGLa and GS behave similarly in many ways, as they (i) prefer their surface-bound state at high temperature, yet (ii) they can favorably re-align and get immersed into the membrane, which (iii) occurs most prominently in a temperature range just above and around the lipid phase transition. For all further experiments, we will thus not only prepare samples with the selected P/L ratio, but we will also acquire all NMR data as temperature-dependent series by stepping up in intervals of 5° from ±10° below to above $T_m$ of the respective lipid.

### 3.3. Influence of lipid acyl chain length

Saturated phosphatidylcholines are conveniently used to study the impact of bilayer thickness on peptide–lipid interactions. In the series DLPC (di-C12:0) → DMPC (di-C14:0) → DPPC (di-C16:0) the acyl chain length successively increases by two methylene units, and the respective $T_m$ values (−1 °C, 23 °C, 41 °C) [61] are within an experimentally accessible range. All of these samples with PGLa and GS gave well-oriented lamellar $^{31}$P NMR spectra (data not shown). Fig. 3 shows that PGLa has a pronounced preference to re-align in thin DLPC bilayers.

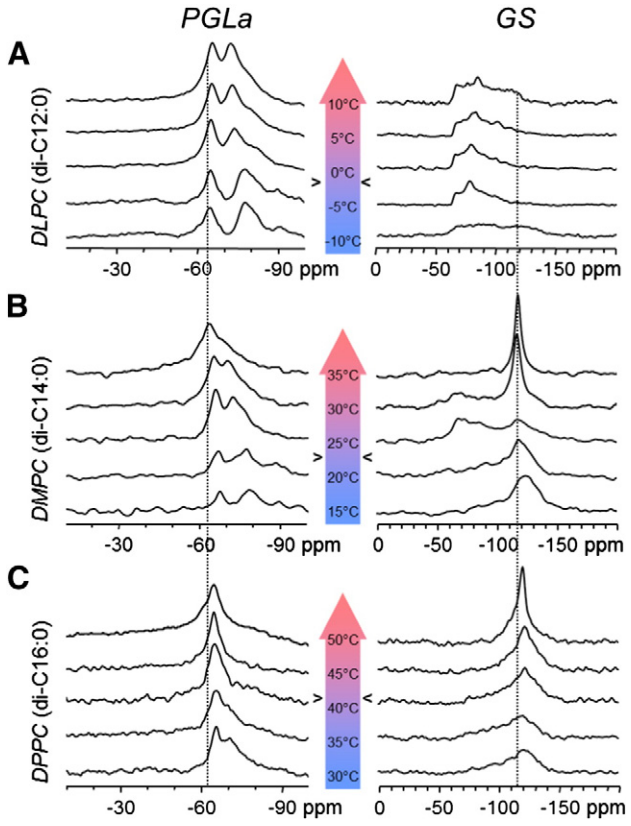


**Fig. 3.** Influence of bilayer thickness on the re-alignment of PGLa (left, P/L = 1:50) and GS (right, P/L = 1:40) in saturated phosphatidylcholines with different acyl chain lengths, measured as a function of temperature. The phase transition temperatures of DLPC ($T_m$ ~ −1 °C) (A), DMPC ($T_m$ ~ 23 °C) (B) and DPPC ($T_m$ ~ 41 °C) (C) are indicated by arrowheads.

Only upfield signals are observed here for the full temperature window scanned over $T_m \pm 10°$. In DMPC, the temperature series corresponds to an excerpt from Fig. 2B, showing successive re-alignment from surface-bound to membrane-immersed with decreasing temperature. Note that fast exchange between the two states of PGLa (time-averaged signal at $\delta_{iso}$) is seen here at the highest temperature of $T_m + 10$ °C. In thick DPPC bilayers, finally, this fast exchange is more pronounced and maintained towards lower temperatures, and full re-alignment is not achieved even at $T_m - 10$ °C. For GS, the same trend is seen as for PGLa, namely that re-alignment occurs most favorably in thin DLPC, and is least favorable in DPPC. In fact, the membrane-inserted state of GS is stabilized in DLPC over a very extended temperature range of about 30° around $T_m$ (full series not shown). In DMPC, GS becomes re-aligned over a modest temperature window of about 15° just above $T_m$, while in DPPC it does not re-align significantly and remains surface-bound over the entire temperature window. We may thus conclude that the two peptides behave similarly with regard to their orientational preferences, because they re-align much more favorably in thin bilayers as compared to thick ones.

### 3.4. Influence of negatively charged lipids

The outer monolayer of eukaryotic plasma membranes contains mostly zwitterionic lipids with choline head groups, which are readily mimicked by phosphocholine model membranes, such as DMPC used here. Bacterial membranes, however, are enriched in negatively charged lipids and attract cationic AMPs electrostatically. PGLa is known to require some anionic lipids in order to bind to vesicles in dilute suspensions [38,62]. Nevertheless, when using macroscopically oriented samples, the peptide has been shown to be fully retained between uncharged DMPC bilayers, as it cannot swim away without any excess water [36,54]. In the present solid state NMR study, we therefore need not be concerned about the initial binding equilibrium. Instead, we

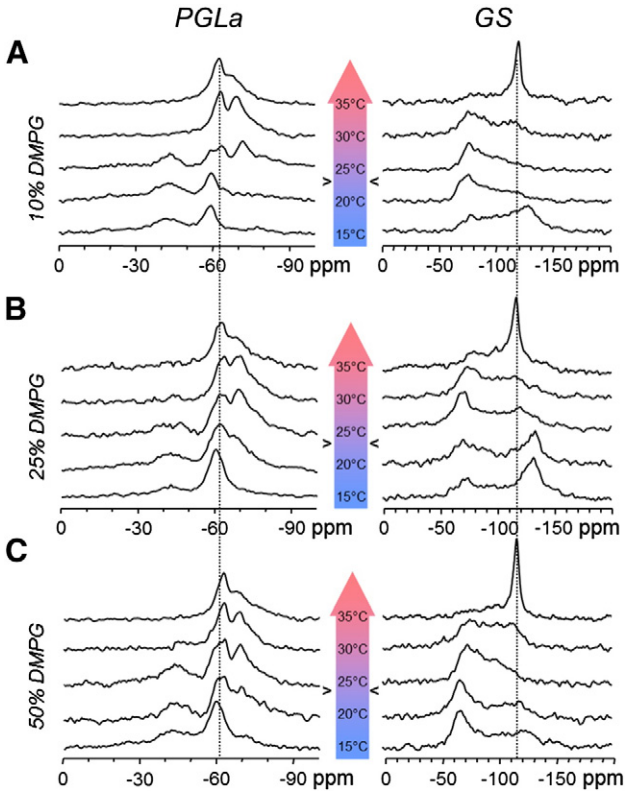


**Fig. 4.** Influence of lipid headgroup charge on the re-alignment of PGLa (left), and GS (right), measured in a DMPC matrix containing 10% anionic DMPG (A), 25% (B), and 50% (C). The lipid phase transition is indicated by arrowheads.

can focus directly on the re-alignment of membrane-bound PGLa and GS, and see how this equilibrium is affected by the presence of 10, 25 and 50% anionic lipid.

It has been previously demonstrated that $^{19}$F-labeled PGLa in oriented samples of pure DMPC gives the same spectra, at identical P/L and comparable temperature conditions, as in the presence of 25% and 50% DMPG [37,38]. It was thus concluded that the structural behavior of PGLa is unaffected by the presence of anionic lipids. However, those experiments were only carried out in fluid liquid crystalline samples, so we now performed a series of temperature scans with mixtures of DMPC and DMPG. The $^{19}$F NMR spectra in Fig. 4 (to be compared with those of pure DMPC in Figs. 2B/3B) show that at temperatures above the $T_m$ the behavior of both PGLa and GS is not affected by the presence of DMPG (10% up to 50%). Below the lipid phase transition, however, a rather different picture emerges, which varies for the two peptides. While PGLa becomes re-aligned in the gel-phase of pure DMPC (upfield signals in Figs. 2B/3B), re-alignment is impaired in the presence of DMPG, which instead seems to stabilize a surface-bound state (downfield signals in Fig. 4A/B/C). In the case of GS, on the other hand, the surface-bound state prevails in the gel-phase of pure DMPC (near-isotropic position in Figs. 2B/3B), but the presence of DMPG below the phase transition temperature promotes the re-aligned state (downfield intensity in Fig. 4A/B/C). The latter effect is nicely seen in the different spectra acquired in the lipid gel phase at −15 °C, where the downfield signal of GS at −70 ppm is absent in pure DMPC, but grows with increasing DMPG content and eventually dominates the spectrum at 50% DMPG. In another series of experiments, spectra were collected with mixtures of anionic DMPS/DMPC (data not shown), and the qualitiative behavior of the two peptides was similar to the data with DMPG/DMPC. We may thus conclude that anionic lipids have no significant effect on the re-alignment of PGLa and GS in the fluid liquid crystalline phase. However, the two peptides exhibit different trends in the lipid gel phase, as it had also been noted in pure DMPC.

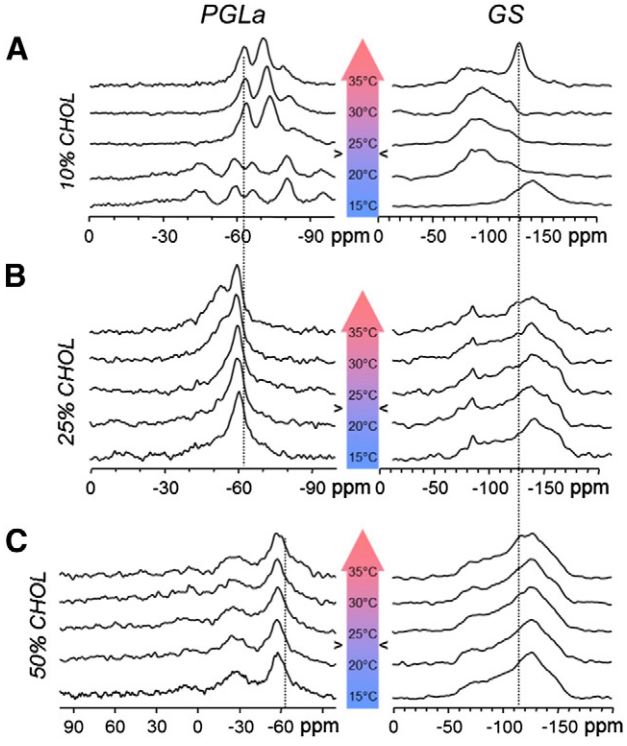


**Fig. 5.** Influence of cholesterol content on the re-alignment of PGLa (left) and GS (right), measured in a DMPC matrix containing 10% CHOL (A), 25% (B), and 50% (C). The lipid phase transition of pure DMPC is indicated by arrowheads. Note the extended ppm scale for PGLa in panel C.

### 3.5. Influence of cholesterol

The presence of cholesterol is a major characteristic that distinguishes animal cell membranes from those of bacteria. High cholesterol content is supposed to be an important factor governing the selectivity of AMPs against prokaryotes *versus* eukaryotes, by sealing the membranes against peptide insertion [13–16,63]. We therefore examined the alignment preferences of PGla and GS in DMPC bilayers containing 10, 25, and 50 mol% cholesterol (CHOL). Again, $^{31}$P NMR confirmed that the lipids were well oriented and in the lamellar phase (data not shown). The representative $^{19}$F NMR spectra of PGLa in Fig. 5A show that a low cholesterol content (10%) keeps the peptide aligned on the membrane surface at temperatures above $T_m$. Below the DMPC phase transition temperature, the well-resolved multicomponent spectra indicate a co-existence of the surface-bound state (downfield signals) and the fully re-aligned state (upfield signals). At higher cholesterol contents (25%), the lipid phase transition is completely smeared out, as expected, and all spectra show just a broad lineshape (Fig. 5B). This develops into an extremely broad triplet pattern at 50% CHOL (Fig. 5C, note the different ppm scale). It appears that PGLa does not bind to these membranes in the usual S-/T-/I-states that were seen above and described in the literature so far. The maximum static $^{19}$F splitting is found in Fig. 5C, similar to a situation reported recently for an amphiphilic β-stranded peptide $[KIGAKI]_3$ [20,21]. We may thus speculate that the PGLa helix could have become unfolded in the presence of 50% CHOL, and might lie immobilized on the membrane surface in an extended conformation [64].

The behavior of GS is more readily interpreted from the distinct NMR lineshapes. Compared to pure DMPC, the re-aligned state is dramatically stabilized by 10% CHOL (Fig. 5A). This membrane composition actually seems to be most effective in promoting the immersed state of GS, compared to all other lipid systems examined here. At higher cholesterol content (25%, 50%), on the other hand, static powder patterns are observed for all temperatures in Fig. 5B/C. In these cholesterol-rich mixtures, the peptide completely loses its orientation. This observation suggests that GS is excluded from the lipid bilayer and/or cannot bind any more in an ordered manner. At the same time $^{31}$P NMR indicates that the phospholipids maintain their high-quality lamellar orientation (data not shown).

### 3.6. Lipid mixtures mimicking bacterial membranes

Apart from the negative charge and the absence of cholesterol, another distinct feature of bacterial membranes is a high content of phosphatidylethanolamines (PE) and cardiolipins (CL). Both of these lipids have a small headgroup and thereby promote negative bilayer curvature [65,66]. Even though these lipids are also present in other cell types, it is often assumed that a bacterial membrane can be modeled as a PE/PG mixture [67]. To figure out how PGLa and GS respond to such an environment, we collected temperature-dependent $^{19}$F NMR spectra in a 1:1 POPE/DMPG[2] mixture. Furthermore, oriented samples were prepared also with a total lipid extract (TLE)[3] from *E. coli*, which should be closer to the native lipid composition than any synthetic mixture. Fig. 6A/B shows that both PGLa and GS are retained in the surface-bound state in these samples throughout all temperatures investigated. Apparently, neither PGLa nor GS are able to re-align in these bacteria-mimicking membranes. This observation supports a recent study in which we had examined PGLa and GS in native biomembranes, prepared from *Micrococcus luteus* bacterial protoplasts and from human

[2] In the POPE/DMPG mixture the individual lipid phase transition temperatures are close to one another (25° and 23 °C, respectively), such that homogeneous bilayers are readily formed. In other acyl chain combinations, poor miscibility and lateral phase separation are expected to severely perturb the homogeneity of the bilayer at ambient temperatures.

[3] The TLE contains approximately 4:1 PE/PG and 10% CL, such that PE/(PG + CL) is about 7:3.

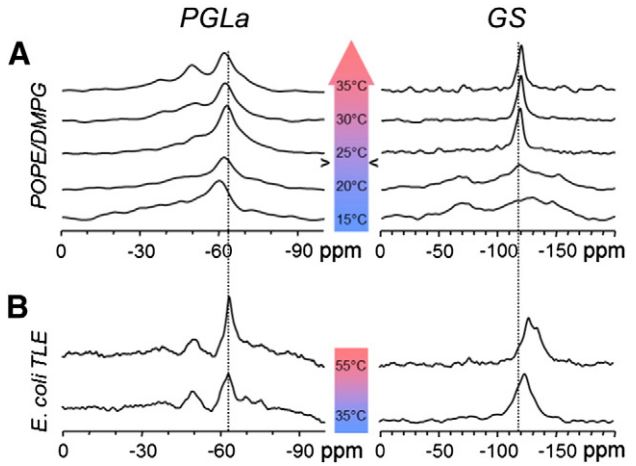


**Fig. 6.** Influence of bacterial membrane-mimicking lipids on the re-alignment of PGLa (left) and GS (right), measured in a POPE/DMPG mixture (A), and in a total lipid extract from *E. coli* (B).

erythrocyte ghosts [29,57]. The peptides showed characteristic fingerprints of the surface-bound states, and re-alignment was not detected in bacterial membranes, but detected in erythrocyte ghosts.

## 4. Discussion

For many years peptide–lipid interactions have been a major focus in studies of antimicrobial peptides. Even though attention is starting to shift towards other modes of intracellular action, involving DNA, RNA, signaling or energy-generating systems, the plasma membrane is still an obligatory interaction partner for AMPs. After all, any peptide will need to break or translocate across this barrier, even if its main target is in the cytosol [68,69]. Therefore, it is important to systematically investigate the basic interactions between different AMPs and different lipids. In this work we have compared the structural behavior of two amphiphilic AMPs with fundamentally different primary and secondary structures: the α-helical PGLa and the cyclic β-stranded gramicidin S, bound to model membranes of varying composition and with different properties (fluid/gel phase, membrane thickness, surface charge, cholesterol content, bilayer curvature). Despite their marked differences in structure and charge, the two amphiphilic AMPs show surprisingly similar re-alignment behaviors, which suggest very similar peptide–lipid interactions as well as similar functional mechanisms towards membrane disruption and/or pore formation. Both of them bind to membranes in a surface-bound state, and can re-align and insert more deeply into the bilayer with increasing concentration [27,37,38,46]. We used solid state $^{19}$F NMR to monitor the alignment states of the peptides by rapidly acquiring "fingerprint" lineshapes. Experiments were carried out to screen peptide concentration (Fig. 2A), temperature (Fig. 2B), and various lipid environments (Figs. 3–6).

Methodologically, the present study may be regarded a as a proof of principle that a single $^{19}$F-reporter group on a peptide can be used for fast and efficient high-through put screen of many different conditions. The spectra presented here do not display perfect lineshapes, and they have not been optimized individually. Nevertheless, they are of sufficient quality to extract the essential information, namely whether the peptide has re-aligned or not, or whether a powder spectrum or something unusual is seen (*e.g.* fast exchange). Within these caveats, we do not attempt to analyze our data quantitatively, but the observed trends are definite and can be reproduced. We typically used 0.5 mg peptide and acquired each spectrum in less than 2 h, which ensures that the sample stays well hydrated [41,53]. Solid state NMR experiments based on conventional isotope labels ($^{2}$H, $^{15}$N) would require larger amounts of peptide (several milligrams) and longer (tens of hours) measurement times. Besides the high cost, such long experiments would also affect the hydration state of an oriented sample, which would inevitably dry out in a temperature series and would in turn shift the lipid phase transition $T_m$ to significantly higher temperatures. This risk was minimized by $^{19}$F NMR, and the sample integrity could be confirmed by $^{31}$P NMR afterwards.

When studied under conditions close to the threshold for re-alignment, we found that both peptides immerse most favorably into phosphatidylcholine membranes at temperatures around the respective lipid phase transition. In model membranes consisting of a single synthetic lipid type, the gel and fluid liquid crystalline phases co-exist as discrete domains at the phase transition temperature $T_m$ [70–72]. Numerous lipid packing defects are present at the domain boundaries, which should facilitate the membrane insertion of a peptide and hence a change in its alignment. This instability at $T_m$ explains why the observed re-alignment of PGLa and GS is coupled to the chain melting transition in synthetic lipid bilayers.

When enriched with cholesterol the lipid phase transition disappears, and cholesterol is considered to act as a membrane "sealer". Accordingly, we saw that ≥25% CHOL impairs the re-alignment of PGLa, and prevents the binding of GS in a well-aligned state altogether (Fig. 5). Remarkably, in the presence of 10% cholesterol we observed a strikingly different behavior for both peptides. PGLa and GS did not only bind strongly to these membranes, but their re-alignment was actively promoted. In fact, the re-alignment of GS was most favorable in the presence of 10% cholesterol in a DMPC matrix, compared to any other lipid composition studied. It is conceivable that cholesterol induces numerous bilayer defects or microdomains in this particular concentration regime [73], where it starts to broaden the phase transition region that is *per se* most sensitive to peptide insertion. Membranes with low cholesterol content might thus be particularly susceptible to membrane-active peptides. This could include, *e.g.*, cholesterol-poor domains in the plasma membrane, but also ER/Golgi membranes, which become accessible to endocytotically acquired cationic peptides.

In bacterial-mimicking lipid mixtures of POPE/DMPG and in *E. coli* total lipid extract, as well as in native biomembranes [29,57], we did not see any re-alignment of either peptide (Fig. 6). From a biological point of view, this finding might be unexpected at first sight, given that AMPs have a high selectivity for bacterial cells [74]. However, our observations are in good agreement with the physico-chemical properties of these lipid systems. Lipids with a high negative curvature have been shown to prevent the immersion of the amphiphilic α-helical peptide MSI-103, which closely resembles PGLa [44]. The present data on PGLa and GS support this curvature concept, as bacterial lipids typically have small headgroups (PE, CL) and bulky unsaturated acyl chains. Such bilayers keep the peptides in the surface-bound state, as – conceptionally – there is much room for them within the headgroup region. Indeed, direct dipolar interactions have been detected between the PG headgroup and the interfacial arginine side chain of human cathelicidin LL-37 and its fragments [75,76]. Lipids with large headgroups and short saturated chains, on the other hand, have a positive spontaneous curvature, which favors the re-alignment and deeper insertion of peptides into the hydrophobic core [44]. Extending the curvature concept further, we may even argue that increasing temperature leads to an increasingly negative curvature of any lipid, as the fluctuating acyls chains will occupy a larger volume. Accordingly, in our present and previous temperature series we always saw that if a peptide had properly re-aligned in a stable state above $T_m$ (*e.g.* at high P/L ratio), it would eventually become surface-bound upon raising the temperature.

Regarding the properties of the lipid acyl chains, we have demonstrated here that both PGLa and GS have the same tendency to re-align favorable in thin DLPC bilayers, less so in DMPC, and not at all in DPPC (when measured under equivalent conditions of appropriate peptide concentrations and relative temperatures, Fig. 3). This series can also be rationalized by the curvature concept, as the lipid curvature decreases with increasing acyl chain volume from DLPC to DMPC to DPPC. Cosequently, the threshold concentrations for re-alignment of

PGLa and GS in DLPC must be below the respective values determined in DMPC (Fig. 2A), while the thresholds in DPPC must be even higher. It would be interesting to verify these expected trends by providing actual numbers. However, the experimental effort to measure such concentration series is considerable, as individual samples would need to be prepared for each spectrum. Instead of scanning peptide concentrations, it is much more convenient to scan the temperature using one and the same sample, which was the main approach taken in this study.

Different peptides obviously have different threshold concentrations for re-alignment, as seen here for PGLa and GS in DMPC at 25 °C (Fig. 2A), and these values will furthermore differ in each and every lipid system studied. Nevertheless, the relative values are shifted by the specific membrane environment in a consistent manner according to the bilayer properties, such as lipid curvature and bilayer defects. With these two exemplary peptides, examined under different conditions (concentration, temperature) and in different types of lipids, we have demonstrated that peptide–lipid interactions are based on fundamental physico-chemical properties of the participating molecules. This particular importance of lipids has been also discussed recently from perspective of the pore formation mechanism [77]. When comparing the effect of different AMPs on different types of cell membranes, it can thus be expected that the actual events at the level of the lipid bilayer proceed in a quantitatively predictable way. On the other hand, the observed biological activities of different peptides against different strains do not necessarily correlate with lipid composition. That is because the "effective" antimicrobial activity will obviously depend on the local concentration that can be achieved for each individual peptide at the cell surface. This initial binding interaction is largely governed by electrostatic attraction to lipids and other cell-surface components, which was not considered here.

For instance, the present study has shown that re-alignment and membrane immersion do not proceed readily in bacterial membranes and mimicking lipid mixtures thereof. The presence of negatively charged head groups has no favorable effect on promoting re-alignment *per se* (Fig. 4), and the typical bacterial lipid PE even hinders peptide immersion due its high negative spontaneous curvature (Fig. 6) [44]. The fact that antimicrobial peptides are nevertheless particularly active against bacterial membranes compared to eukaryotic ones, must therefore be attributed purely to strong electrostatic attraction. In order to permeabilize a bacterial cell, it is likely that much higher peptide concentrations are needed than the P/L ratios at which re-alignment in model bilayers was observed. From a quantitative point of view, it is important to note that the peptide concentrations used here (P/L of 1:20 to 1:200) are far below the corresponding MIC values. By considering the average surface area ($2 \times 4\,\mu m^2$) of all bacteria in an antimicrobial assay, it was estimated that a typical MIC of 8 μg/ml corresponds to a nominal P/L ratio > 1:1 [78]. Compared to the concentrations that would be present, even if only a fraction of the peptides binds to the membrane at a given time, we have thus monitored sub-MIC effects here. The surprisingly unfavorable tendency for PGLa and GS to undergo re-alignment in bacterial-mimicking lipid mixtures thus has to be compensated *in vivo* by a high local peptide concentration attracted electrostatically. On the other hand, the number of pores needed to kill a bacterial cell does not need to be very large [79], and only a small fraction of the membrane-bound molecules may be involved in a transient event. In an NMR experiment, such a small but sufficient population of active, re-aligned structures may be too low for observation under realistic conditions.

Overall, we have shown that the two amphiphilic peptides PGLa (α-helical 21mer, charge +5) and gramicidin S (cyclic β-pleated decamer, charge +2) resemble each other closely in their re-alignment behavior, once their respective threshold concentrations for membrane immersion is taken into account. Their functional mechanism therefore seems to be determined in a very similar way by the physico-chemical parameters of the lipid system. These observations suggest that it is not the peptide *per se*, but rather the phase state and lipid composition of the target cell membrane that influence the re-alignment and membrane insertion of antimicrobial peptides.

## Acknowledgements

We acknowledge the DFG-Center for Functional Nanostructures (TP E1.2). JS acknowledges support by the Spanish MINECO (BFU2010-19118, financed in part by the European Regional Development Fund).

## References

[1] M. Zasloff, Antimicrobial peptides of multicellular organisms, Nature 415 (2002) 389–395.
[2] L.M. Rossi, P. Rangsamy, J. Zhang, X.Q. Qiu, G.Y. Wu, Research advances in the development of peptide antibiotics, J. Pharm. Sci. 97 (2008) 1060–1070.
[3] A.R. Koczulla, R. Bals, Antimicrobial peptides: current status and therapeutic potential, Drugs 63 (2003) 389–406.
[4] L. Kuhn-Nentwig, Antimicrobial and cytolytic peptides of venomous arthropods, Cell. Mol. Life Sci. 60 (2003) 2651–2668.
[5] E. de Leeuw, W. Lu, Human defensins: turning defense into offense, Infect. Disord. Drug Targets 7 (2007) 67–70.
[6] N.P. West, D.B. Pyne, G. Renshaw, A.W. Cripps, Antimicrobial peptides and proteins, exercise and innate mucosal immunity, FEMS Immunol. Med. Microbiol. 48 (2006) 293–304.
[7] J. Harder, R. Glaser, J.M. Schroder, The role and potential therapeutical applications of antimicrobial proteins in infectious and inflammatory diseases, Endocr. Metab. Immune Disord. Drug Targets 7 (2007) 75–82.
[8] K.L. Brown, R.E.W. Hancock, Cationic host defense (antimicrobial) peptides, Curr. Opin. Immunol. 18 (2006) 24–30.
[9] H. Jenssen, P. Hamill, R.E.W. Hancock, Peptide antimicrobial agents, Clin. Microbiol. Rev. 19 (2006) 491–511.
[10] R.E.W. Hancock, A. Rozek, Role of membranes in the activities of antimicrobial cationic peptides, FEMS Microbiol. Lett. 206 (2002) 143–149.
[11] D. Wade, A. Boman, B. Wahlin, C.M. Drain, D. Andreu, H.G. Boman, R.B. Merrifield, All-D amino acid-containing channel-forming antibiotic peptides, Proc. Natl. Acad. Sci. U. S. A. 87 (1990) 4761–4765.
[12] R. Bessalle, A. Kapitkovsky, A. Gorea, I. Shalit, M. Fridkin, All-D-magainin: chirality, antimicrobial activity and proteolytic resistance, FEBS Lett. 274 (1990) 151–155.
[13] N. Papo, Y. Shai, Can we predict biological activity of antimicrobial peptides from their interactions with model phospholipid membranes? Peptides 24 (2003) 1693–1703.
[14] E. Glukhov, M. Stark, L.L. Burrows, C.M. Deber, Basis for selectivity of cationic antimicrobial peptides for bacterial versus mammalian membranes, J. Biol. Chem. 280 (2005) 33960–33967.
[15] R.M. Epand, R.F. Epand, Bacterial membrane lipids in the action of antimicrobial agents, J. Pept. Sci. 17 (2011) 298–305.
[16] K. Matsuzaki, K. Sugishita, N. Fujii, K. Miyajima, Molecular basis for membrane selectivity of an antimicrobial peptide, magainin 2, Biochemistry 34 (1995) 3423–3429.
[17] K. Matsuzaki, Why and how are peptide–lipid interactions utilized for self-defense? Magainins and tachyplesins as archetypes, Biochim. Biophys. Acta 1462 (1999) 1–10.
[18] Y. Shai, Mechanism of the binding, insertion and destabilization of phospholipid bilayer membranes by α-helical antimicrobial and cell non-selective membrane-lytic peptides, Biochim. Biophys. Acta 1462 (1999) 55–70.
[19] L. Yang, T.M. Weiss, R.I. Lehrer, H.W. Huang, Crystallization of antimicrobial pores in membranes: magainin and protegrin, Biophys. J. 79 (2000) 2002–2009.
[20] P. Wadhwani, J. Bürck, E. Strandberg, C. Mink, S. Afonin, M. Ieronimo, A.S. Ulrich, Using a sterically restrictive amino acid as a $^{19}$F NMR label to monitor and to control peptide aggregation in membranes, J. Am. Chem. Soc. 130 (2008) 16515–16517.
[21] P. Wadhwani, E. Strandberg, N. Heidenreich, J. Bürck, S. Fanghänel, A.S. Ulrich, Self-assembly of flexible β-strands into immobile amyloid-like β-sheets in membranes as revealed by solid-state $^{19}$ F NMR, J. Am. Chem. Soc. 134 (2012) 6512–6515.
[22] P. Wadhwani, J. Reichert, E. Strandberg, J. Bürck, J. Misiewicz, S. Afonin, N. Heidenreich, S. Fanghänel, P.K. Mykhailiuk, I.V. Komarov, A.S. Ulrich, Stereochemical effects on the aggregation and biological properties of the fibril-forming peptide $[KIGAKI]_3$ in membranes, Phys. Chem. Chem. Phys. 15 (2013) 8962–8971.
[23] E. Strandberg, A.S. Ulrich, NMR methods for studying membrane-active antimicrobial peptides, Concepts Magn. Reson. A 23A (2004) 89–120.
[24] A.S. Ulrich, Solid state $^{19}$F NMR methods for studying biomembranes, Prog. NMR Spectr. 46 (2005) 1–21.
[25] A. Drechsler, F. Separovic, Solid-state NMR structure determination, IUBMB Life. 55 (2003) 515–523.
[26] M. Hong, Oligomeric structure, dynamics, and orientation of membrane proteins from solid-state NMR, Structure 14 (2006) 1731–1740.
[27] A.S. Ulrich, P. Wadhwani, U.H.N. Dürr, S. Afonin, R.W. Glaser, E. Strandberg, P. Tremouilhac, C. Sachse, M. Berditchevskaia, S.L. Grage, Solid-state $^{19}$F-nuclear magnetic resonance analysis of membrane-active peptides, in: A. Ramamoorthy (Ed.), NMR Spectroscopy of Biological Solids, Taylor & Francis, 2006, pp. 215–236.
[28] P. Wadhwani, P. Tremouilhac, E. Strandberg, S. Afonin, S.L. Grage, M. Ieronimo, M. Berditsch, A.S. Ulrich, Using fluorinated amino acids for structure analysis of membrane-active peptides by solid-state $^{19}$F-NMR, in: V. Soloshonok, K. Mikami, T. Yamazaki, J.T. Welch, J. Honek (Eds.), Current Fluoroorganic Chemistry, American Chemical Society, Washington, DC, 2007.
[29] K. Koch, S. Afonin, M. Ieronimo, M. Berditsch, A.S. Ulrich, Solid-state $^{19}$F-NMR of peptides in native membranes, Top. Curr. Chem. 306 (2008) 89–118.
[30] V.S. Kubyshkin, I.V. Komarov, S. Afonin, P.K. Mykhailiuk, S.L. Grage, A.S. Ulrich, Trifluoromethyl-substituted α-amino acids as solid state $^{19}$F-NMR labels for structural studies of membrane-bound peptides, in: V. Gouverneur, K. Müller

(Eds.), Fluorine in Pharmaceutical and Medicinal Chemistry: From Biophysical Aspects to Clinical Applications, Imperial College Press, 2012, pp. 91–138.
[31] M. Auger, Biological membrane structure by solid-state NMR, Curr. Issues Mol. Biol. 2 (2000) 119–124.
[32] J. Seelig, $^{31}$P nuclear magnetic resonance and the head group structure of phospholipids in membranes, Biochim. Biophys. Acta 515 (1978) 105–140.
[33] A. Ramamoorthy, Preface, Biochim. Biophys. Acta 1758 (2006) 1177 (and titles there in, Special issue "Membrane Biophysics of Antimicrobial Peptides").
[34] S. Afonin, D. Juretić, F. Separovic, A.S. Ulrich, Special issue on membrane-active peptides, Eur. Biophys. J. 40 (2011) 347–348 (and titles there in, Special issue on membrane-active peptides).
[35] S.L. Grage, S. Afonin, A.S. Ulrich, Dynamic transitions of membrane-active peptides, Methods Mol. Biol. 618 (2010) 183–207.
[36] R.W. Glaser, C. Sachse, U.H.N. Dürr, P. Wadhwani, A.S. Ulrich, Orientation of the antimicrobial peptide PGLa in lipid membranes determined from $^{19}$F-NMR dipolar couplings of 4-$CF_3$-phenylglycine labels, J. Magn. Reson. 168 (2004) 153–163.
[37] R.W. Glaser, C. Sachse, U.H.N. Dürr, P. Wadhwani, S. Afonin, E. Strandberg, A.S. Ulrich, Concentration-dependent realignment of the antimicrobial peptide PGLa in lipid membranes observed by solid-state $^{19}$F-NMR, Biophys. J. 88 (2005) 3392–3397.
[38] P. Tremouilhac, E. Strandberg, P. Wadwhani, A.S. Ulrich, Conditions affecting the re-alignment of the antimicrobial peptide PGLa in membranes as monitored by solid state $^2$H-NMR, Biochim. Biophys. Acta 1758 (2006) 1330–1342.
[39] P. Tremouilhac, E. Strandberg, P. Wadhwani, A.S. Ulrich, Synergistic transmembrane alignment of the antimicrobial heterodimer PGLa/magainin, J. Biol. Chem. 281 (2006) 32089–32094.
[40] J. Bürck, S. Roth, P. Wadhwani, S. Afonin, N. Kanithasen, E. Strandberg, A.S. Ulrich, Conformation and membrane orientation of amphiphilic helical peptides by oriented circular dichroism, Biophys. J. 95 (2008) 3872–3881.
[41] S. Afonin, S.L. Grage, M. Ieronimo, P. Wadhwani, A.S. Ulrich, Temperature-dependent transmembrane insertion of the amphiphilic peptide PGLa in lipid bilayers observed by solid state $^{19}$F NMR spectroscopy, J. Am. Chem. Soc. 130 (2008) 16512–16514.
[42] E. Strandberg, P. Tremouilhac, P. Wadhwani, A.S. Ulrich, Synergistic transmembrane insertion of the heterodimeric PGLa/magainin 2 complex studied by solid-state NMR, Biochim. Biophys. Acta 1788 (2009) 1667–1679.
[43] E. Strandberg, J. Zerweck, P. Wadhwani, A.S. Ulrich, Synergistic insertion of antimicrobial magainin-family peptides in membranes depends on the lipid spontaneous curvature, Biophys. J. 104 (2013) L9–L11.
[44] E. Strandberg, D. Tiltak, S. Ehni, P. Wadhwani, A.S. Ulrich, Lipid shape is a key factor for membrane interactions of amphipathic helical peptides, Biochim. Biophys. Acta 1818 (2012) 1764–1776.
[45] J. Salgado, S.L. Grage, L.H. Kondejewski, R.S. Hodges, R.N. McElhaney, A.S. Ulrich, Membrane-bound structure and alignment of the antimicrobial β-sheet peptide gramicidin S derived from angular and distance constraints by solid state $^{19}$F-NMR, J. Biomol. NMR 21 (2001) 191–208.
[46] S. Afonin, U.H.N. Dürr, P. Wadhwani, J. Salgado, A.S. Ulrich, Solid state NMR structure analysis of the antimicrobial peptide gramicidin s in lipid membranes: concentration-dependent re-alignment and self-assembly as a β-barrel, Top. Curr. Chem. 273 (2008) 139–154.
[47] W.L. Maloy, U.P. Kari, Structure-activity studies on magainins and other host defense peptides, Biopolymers 37 (1995) 105–122.
[48] J.P. Ulmschneider, J.C. Smith, M.B. Ulmschneider, A.S. Ulrich, E. Strandberg, Reorientation and dimerization of the membrane-bound antimicrobial peptide PGLa from microsecond all-atom MD simulations, Biophys. J. 103 (2012) 472–482.
[49] Wang et al. in "current issue of BBA".
[50] M. Berditsch, S. Afonin, A.S. Ulrich, The ability of *Aneurinibacillus migulanus* (*Bacillus brevis*) to produce the antibiotic gramicidin S is correlated with phenotype variation, Appl. Environ. Microbiol. 73 (2007) 6620–6628.
[51] G.G. Gause, M.G. Brazhnikova, Gramicidin S and its use in the treatment of infected wounds, Nature 154 (1944) 703.
[52] N. Izumiya, T. Kato, H. Aoyaga, M. Waki, M. Kondo, Synthetic Aspects of Biologically Active Cyclic Peptides: Gramicidin S and Tyrocidines, Halsted Press, NY, 1979.
[53] S. Afonin, P.K. Mikhailiuk, I.V. Komarov, A.S. Ulrich, Evaluating the amino acid $CF_3$-bicyclopentylglycine as a new label for solid-state $^{19}$F-NMR structure analysis of membrane-bound peptides, J. Pept. Sci. 13 (2007) 614–623.
[54] S. Afonin, R.W. Glaser, M. Berditchevskaia, P. Wadhwani, K.H. Gührs, U. Möllmann, A. Perner, A.S. Ulrich, 4-Fluorophenylglycine as a label for $^{19}$F NMR structure analysis of membrane-associated peptides, ChemBioChem 4 (2003) 1151–1163.
[55] P.K. Mikhailiuk, S. Afonin, A.N. Chernega, E.B. Rusanov, M.O. Platonov, G.G. Dubinina, M. Berditsch, A.S. Ulrich, I.V. Komarov, Conformationally rigid trifluoromethyl-substituted α-amino acid designed for peptide structure analysis by solid-state $^{19}$ F NMR spectroscopy, Angew. Chem. Int. Ed. 45 (2006) 5659–5661.
[56] E. Strandberg, P. Wadhwani, P. Tremouilhac, U.H.N. Dürr, A.S. Ulrich, Solid-state NMR analysis of the PGLa peptide orientation in DMPC bilayers: structural fidelity of $^2$H-labels versus high sensitivity of $^{19}$F-NMR, Biophys. J. 90 (2006) 1676–1686.
[57] M. Ieronimo, S. Afonin, K. Koch, M. Berditsch, P. Wadhwani, A.S. Ulrich, $^{19}$F NMR analysis of the antimicrobial peptide PGLa bound to native cell membranes from bacterial protoplasts and human erythrocytes, J. Am. Chem. Soc. 132 (2010) 8822–8824.
[58] P. Wadhwani, S. Afonin, M. Ieronimo, J. Buerck, A.S. Ulrich, Optimized protocol for synthesis of cyclic gramicidin S: starting amino acid is key to high yield, J. Org. Chem. 71 (2006) 55–61.
[59] A.L. van Geet, Calibration of methanol nuclear magnetic resonance thermometer at low temperature, Anal. Chem. 42 (1970) 679–680.
[60] R.W. Glaser, A.S. Ulrich, Susceptibility corrections in solid-state NMR experiments with oriented membrane samples. Part I: Applications, J. Magn. Reson. 164 (2003) 104–114.
[61] R. Koynova, M. Caffrey, Phases and phase transitions of the phosphatidylcholines, Biochim. Biophys. Acta 1376 (1998) 91–145.
[62] A. Latal, G. Degovics, R.F. Epand, R.M. Epand, K. Lohner, Structural aspects of the interaction of peptidyl-glycylleucine-carboxyamide, a highly potent antimicrobial peptide from frog skin, with lipids, Eur. J. Biochem. 248 (1997) 938–946.
[63] K. Lohner, S.E. Blondelle, Molecular mechanisms of membrane perturbation by antimicrobial peptides and the use of biophysical studies in the design of novel peptide antibiotics, Comb. Chem. High Throughput Screen. 8 (2005) 241–256.
[64] R.W. Williams, R. Starman, K.M. Taylor, K. Gable, T. Beeler, M. Zasloff, D. Covell, Raman spectroscopy of synthetic antimicrobial frog peptides magainin 2a and PGLa, Biochemistry 29 (1990) 4490–4496.
[65] J. Šajbidor, Effect of some environmental factors on the content and composition of microbial membrane lipids, Crit. Rev. Biotechnol. 17 (1997) 87–103.
[66] P.R. Cullis, B. de Kruijff, Lipid polymorphism and the functional roles of lipids in biological membranes, Biochim. Biophys. Acta 559 (1979) 399–420.
[67] R.M. Epand, R.F. Epand, Domains in bacterial membranes and the action of antimicrobial agents, Mol. Biosyst. 5 (2009) 580–587.
[68] M. Cudic, L. Otvos Jr., Intracellular targets of antibacterial peptides, Curr. Drug Targets 3 (2002) 101–106.
[69] K.A. Brogden, Antimicrobial peptides: pore formers or metabolic inhibitors in bacteria? Nat. Rev. Microbiol. 3 (2005) 238–250.
[70] M.C. Blok, E.C. van der Neut-Kok, L.L. van Deenen, J. de Gier, The effect of chain length and lipid phase transitions on the selective permeability properties of liposomes, Biochim. Biophys. Acta 406 (1975) 187–196.
[71] S.W. Hui, Geometry of phase-separated domains in phospholipid bilayers by diffraction-contrast electron microscopy, Biophys. J. 34 (1981) 383–395.
[72] H.J. Muller, M. Luxnat, H.J. Galla, Lateral diffusion of small solutes and partition of amphipaths in defect structures of lipid bilayers, Biochim. Biophys. Acta 856 (1986) 283–289.
[73] M.C. Rheinstädter, O.G. Mouritsen, Small-scale structure in fluid cholesterol-lipid bilayers, Curr. Opin. Colloid Interface 18 (2013) 440–447.
[74] K. Matsuzaki, Control of cell selectivity of antimicrobial peptides, Biochim. Biophys. Acta 1788 (2009) 1687–1692.
[75] G. Wang, Determination of solution structure and lipid micelle location of an engineered membrane peptide by using one NMR experiment and one sample, Biochim. Biophys. Acta 1768 (2007) 3271–3281.
[76] G. Wang, Structures of human host defense cathelicidin LL-37 and its smallest antimicrobial peptide KR-12 in lipid micelles, J. Biol. Chem. 283 (2009) 32637–32643.
[77] G. Fuertes, D. Giménez, S. Esteban-Martín, O.L. Sánchez-Muñoz, J. Salgado, A lipocentric view of peptide-induced pores, Eur. Biophys. J. 40 (2011) 399–415.
[78] J. Blazyk, R. Wiegand, J. Klein, J. Hammer, R.M. Epand, R.F. Epand, W.L. Maloy, U.P. Kari, A novel linear amphipathic β-sheet cationic antimicrobial peptide with enhanced selectivity for bacterial lipids, J. Biol. Chem. 276 (2001) 27899–27906.
[79] D. Bolintineanu, E. Hazrati, T.H. Davis, R.I. Lehrer, Y.N. Kaznessis, Antimicrobial mechanism of pore-forming protegrin peptides: 100 pores to kill *E. coli*, Peptides 31 (2010) 1–8